JOURNAL OF MATERIALS SCIENCE **34** (1999) 2685–2694

Preparation and properties of alumina-baria nano-composites

B. DJURIČIĆ, S. PICKERING, D. MCGARRY
Institute for Advanced Materials, Joint Research Centre, 1755 ZG Petten, The Netherlands
E-mail: pickering@jrc.nl

Barium doped alumina was prepared by calcination of gels obtained from metal chloride solutions by homogeneous precipitation with urea. The gels were either air-dried, oven-dried, microwave-dried or autoclave treated. The materials were analysed by SAXS, XRD, DTA/TG and TEM. The phase composition of the calcined products depended on the gel drying procedure. Barium aluminates formed directly at low temperatures in the microwave treated gel because of the uniform distribution of barium in the dried gel. After calcination at 1200 °C the aluminates were uniformly distributed as nanoscale particles within an α-Al_2O_3 matrix. In contrast, autoclave treated samples initially consisted of boehmite crystals coated with barium carbonate which reacted on calcination to form a surface layer of $BaAl_2O_4$. The autoclaved material withstood 1 h at 1400 °C in air without transformation to α-Al_2O_3. This increased thermal stability of transition alumina (θ-Al_2O_3) is attributed to the presence of the $BaAl_2O_4$ surface layer. The final transformation to α-Al_2O_3 was associated with the transformation of a surface layer of $BaAl_2O_4$ to nanoscale particles of $BaAl_{9.2}O_{14.8}$.

1. Introduction

Rapid developments in combustion technology coupled with the increasing demands for reduced levels of pollutants emitted by combustion processes has created a demand for new catalyst materials. In particular, new catalysts are needed for temperatures above 1000 °C, not only for the removal of pollutants, e.g. to clean up automobile exhausts, but also for catalytic combustion e.g. in heaters, boilers, and gas turbines [1, 2]. The catalytic combustion of fuels offers the advantages of a more uniform combustion temperature and a more complete combustion of the fuel. The result is a higher thermal efficiency, together with less nitrogen oxide formation through the prevention of localised high temperature areas. Cordierite ($2MgO \cdot 2Al_2O_3 \cdot 5SiO_2$) is used as the catalyst support material in both the types of application mentioned above. A cordierite honeycomb structure with 400 channels/sq. in. coated with a washcoat of high surface area gamma alumina catalyst carrier containing nanoscale noble metal particles is most frequently used. Although cordierite can be used at temperatures up to about 1400 °C, the catalyst carrier washcoat is limited to about 1000 °C by the tendency of gamma alumina to transform to alpha alumina with a dramatic loss of specific surface area. Therefore, to fully exploit the potential of existing cordierite honeycomb structures, catalyst carriers are required that can operate for long periods at temperatures to approximately 1350 °C without a significant decrease of specific surface area due to phase transformation and sintering.

Some oxides with the perovskite type of structure can maintain a high specific surface area at temperatures above 1000 °C [3–5] and are therefore potential high temperature catalyst carrier materials. Barium hexaaluminate, $BaO \cdot 6Al_2O_3$, is one of the most attractive of these materials [6–8]. The crystal structures of barium hexaaluminates are complex and have been described as intermediate between magnetoplumbite (MP) and the β-alumina structures [9–16]. The β-alumina and magnetoplumbite structures consists of "spinel blocks" composed of Al^{3+} and O^{2-} ions and "conducting layers" in which cations other than Al^{3+} are accommodated. The conducting layer has a plane of mirror symmetry and the main difference between the β-alumina and magnetoplumbite structures consists in the number of cations and their arrangement within this layer. The large Ba^{2+} ion preferentially forms the β-alumina type of structure.

Barium hexaaluminate derived from the corresponding alkoxide precursors retained a specific surface area of approximately 10 $m^2\,g^{-1}$ after calcination at 1450 °C for 1 hour [3]. The mechanism proposed for the formation of barium hexaaluminate from alkoxide precursors is the direct formation from an amorphous gel structure where components are mixed on a molecular scale. However, there is no direct experimental evidence for the existence of the mixed aluminium-barium hydroxide or related compounds. It was postulated that the formation of barium hexaaluminate from $BaCO_3$ and γ-alumina occurred via a solid-state reaction in which $BaAl_2O_4$ forms as an intermediate product before transforming to a low specific surface area barium hexaaluminate [3] and it was suggested that it would be necessary to form barium aluminates at low

temperatures to obtain a large specific surface area [5]. In contrast, other authors reported that the formation of $BaAl_2O_4$ as an intermediate product does not necessarily preclude the formation of barium hexaaluminate structures with high specific surface area [4]. However, all authors emphasised that a very fine scale distribution of barium in γ-Al_2O_3 was as a crucial factor for obtaining a high specific surface area in barium hexaaluminate [3–5]. The mechanism of barium hexaaluminate formation and the effect of the barium doping on the stability of transition aluminas in the Al_2O_3-BaO system needs to be better understood if barium hexaaluminates are to be tailored for high temperature catalysts applications or for other applications such as phosphors based on cation-substituted barium hexaaluminates.

The alkoxide route is of limited industrial interest, however, because of the relatively high price of alkoxide reagents. Conventional low cost methods such as powder blending, e.g. of γ-Al_2O_3 and $BaCO_3$ powders, cannot achieve the very fine scale distribution that is required. There is therefore a need for inexpensive and industrially relevant methods for the low-temperature synthesis of the barium-doped alumina and barium hexaaluminates.

In this paper we describe the synthesis of alumina doped with the equivalent of 10 mol % BaO by homogeneous precipitation induced by the thermal decomposition of urea in an aqueous solution of barium and aluminium chlorides. The dependence of the structural and textural properties of the product on the synthesis parameters and on the dehydration and calcination treatment of the gel were investigated. The structural and textural characteristics of the gel, and of the dried and calcined products, were characterised by Small-Angle X-ray Scattering (SAXS), Transmission Electron Microscopy (TEM), High Resolution Transmission Electron Microscopy (HRTEM), and by X-ray diffraction (XRD)—both "*in-situ*" and conventional X-ray diffraction. Finally, we discuss the mechanisms of formation of the various baria aluminates.

2. Experimental

2.1. Materials

Aluminium chloride hexahydrate ($AlCl_3 \cdot 6H_2O$) (Merck, crystalline, purified), barium chloride dihydrate ($BaCl_2 \cdot 2H_2O$) (Baker, analysed, reagent grade), urea (CON_2H_4) (Acros, p.a.) and polyvinylpyrrolidone (PVP, Aldrich, K-30, special grade) were used as received. Solutions of the above reagents were filtered before use.

2.2. Method of gel synthesis

Alumina and alumina doped with 10 mol % baria were synthesised by homogeneous precipitation from metal salt solution induced by the thermal decomposition of urea—see Fig. 1. On heating the solution to 86 °C, the urea decomposed to produce a controlled and uniform increase in pH until precipitation occurred. Similar methods were previously used to synthesise various fine sols and ceramic powders [17–20] and for the coating of ceramic powders with nanolayers of a second phase [21, 22]. Very fine sol particles sedimented from the solution after standing for several hours at room temperature. The reaction product was centrifuged to separate the characteristically voluminous and transparent gel. The gel was washed twice with double its own volume of distilled water to remove most of anion and organic impurities. About 1200 ml of the transparent gel was produced from 5 l of solution in a typical experiment.

Some Ba^{2+} was detected qualitatively in the washing water by precipitation with SO_4^{2-}. The loss of barium

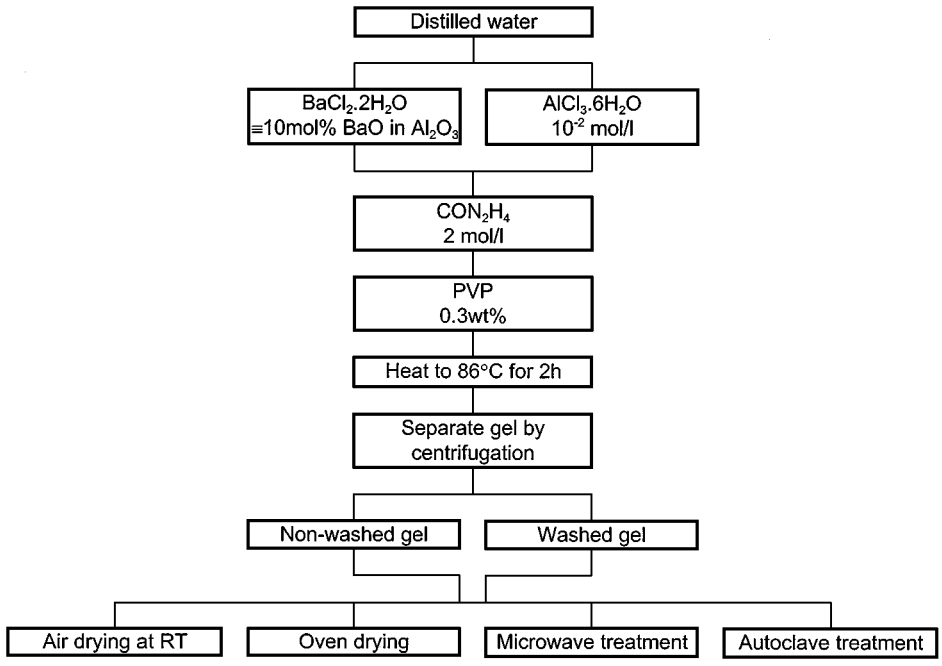

Figure 1 Flow chart of synthesis procedure for alumina-baria precursor gels.

could be avoided by omitting the washing step, in which case the chloride anion was removed by sublimation of NH_4Cl, either during microwave drying, or during calcination in the case of the oven-dried specimens. For autoclave treated gels, washing carried out after crystallisation of boehmite and barium carbonate removed chloride ions without loss of barium.

2.3. Methods for preparing powder from the gel

The alumina and alumina-baria gels were treated in a variety of different ways: air-dried at room temperature, oven-dried at 90–100 °C, dried in a microwave oven, and hydrothermally treated in an autoclave. The air-dried gel was prepared by leaving the gel in a glass beaker at room temperature until a solid formed which was then crushed in an agate mortar to produce a fine powder. The oven-dried gel was prepared by heating the gel in air in an oven at about 90–100 °C for 24 hours; the solid was then crushed as above to produce a fine powder. The microwave-dried samples of gel were prepared in a standard domestic microwave oven at a power setting of 500 W using cycles of: 5 min power on and 2–3 min power off, because of extensive foaming of the gel due to the release of gaseous products. The dried solid was crushed as above and later calcined at different temperatures. Hydrothermal treatment was conducted on 150 ml samples of centrifuged gel in 230 ml Teflon-lined pressure-tight steel containers. A heating rate of about 0.5 °C/min to a temperature of 210 ± 5 °C was used. The hold time at temperature was 4 hours. The resulting brownish liquor with a pH in the range 8–8.5 was decanted and the crystallised product was dried at 90–100 °C. The crystalline product was calcined in either air or argon.

3. Characterisation

The size of the colloidal particles in the alumina and alumina-baria gels was measured by Small Angle X-ray Scattering (SAXS); evaluation of the results of this technique was based on the assumption that the gel was a fractal system [23]. The phase composition of the samples was determined by XRD, either in-situ during calcination (Siemens D5000), or conventionally before and after calcination at various temperatures (Philips PW173). Thermal decomposition of the gel to the calcined products on heating to 1400 °C was observed by differential thermal analysis and thermogravimetry (DTA/TG, Netsch Simultaneous Analyzer STA 409). Transmission electron microscopy (TEM, Philips EM 400) and High Resolution Transmission Electron Microscopy (HRTEM, JEOL 4000 EX/II with a point resolution of 0.165 nm at 400 kV) were used for analysis of the fine structure of uncalcined and calcined samples. Electron microscopy samples were prepared by dispersing the powder in ethyl alcohol, placing a drop of this suspension on a carbon-coated copper grid, and allowing the alcohol to evaporate. The specific surface area was measured by BET nitrogen adsorption (Coulter-Omnisorp 360).

4. Results

4.1. Precipitation of uniform colloidal particles

The important characteristic of the homogeneous precipitation process was that it yielded a product uniform both in chemical composition and particle size. The decomposition of urea on heating the solution released ammonium ions into solution in a very uniform manner resulting in a gradual and uniform increase in pH. These uniform conditions ensured that the alumina-baria composite gel which precipitated from the dissolved chloride salts was chemically homogeneous on a colloidal scale. The precipitation kinetics were easily controlled through the heating rate and the ageing temperature. The flow chart in Fig. 1 summarises the steps and conditions of the synthesis. The size of the sol particles in the gel samples was calculated from SAXS measurements as shown in Table I. The alumina and alumina-baria precursor gels both consisted of particles of about 4 nm diameter and the fractal dimension indicates that both gels were in a similar state of aggregation.

4.2. XRD measurement of phase composition evolution during calcination

The phase evolution during calcination was studied by X-ray diffraction "*in-situ*" and conventionally i.e. on specimens measured at room temperature after calcination. The main results for the conventional measurements are summarised in Table II with phases listed in order of abundance. The phases in alumina-baria samples were compared with those in pure alumina samples to obtain information on the effects of each of the gel treatment techniques.

The alumina-baria gel dried at room temperature appeared to be amorphous from the XRD spectra. The only indication of the presence of a crystalline phases was a small amount of retained urea. The XRD spectrum for the oven-dried sample (100 °C) also indicated predominantly amorphous material XRD and the presence of very poorly crystallized bayerite $Al(OH)_3$ besides traces of crystalline urea. There was no indication of the presence of any crystalline barium containing phase.

In the microwave-treated alumina sample, "*in situ*" XRD indicated the presence of microcrystalline boehmite to approximately 400 °C at which temperature the sample become amorphous and remained amorphous to about 800–850 °C when transition alumina (γ-Al_2O_3) appeared. At about 950–1000 °C transformation of γ-Al_2O_3 to α-Al_2O_3 began and was almost complete at 1200 °C. In the microwave-treated alumina-baria

TABLE I Properties of alumina and alumina-baria precursor gel measured by SAXS

	Alumina	Alumina-baria
Fractal dimension	2.2	2.4
Particle diameter (nm)	3.7	4.1

TABLE II Phase composition of alumina-baria samples before and after calcination of dehydrated gel

	Phases determined by XRD				
	Air				Argon
Sample	Uncalcined	1000 °C/1 h	1200 °C/1 h	1400 °C/1 h	1400 °C/1 h
Oven dried (100 °C/24 h)	Amorphous bayerite urea (tr)	γ-Al_2O_3 BaO	α-Al_2O_3 $BaAl_2O_4$ β_I	α-Al_2O_3 β_I	nd
Microwave dried	Amorphous boehmite $BaAl_{12}O_{19}$ (i)	γ-Al_2O_3 β_{II} (tr)	α-Al_2O_3 θ-Al_2O_3 β_I	α-Al_2O_3 β_I	α-Al_2O_3 β_I
Autoclaved 4 h	Boehmite $BaCO_3$ (i)	γ-Al_2O_3 δ-Al_2O_3 BaO (i)	θ-Al_2O_3 δ-Al_2O_3 $BaAl_2O_4$	θ-Al_2O_3 δ-Al_2O_3 $BaAl_2O_4$ β_{II}	α-Al_2O_3 θ-Al_2O_3 $BaAl_{12}O_{19}$

$\beta_I = BaAl_{13.2}O_{20.8}$, $(BaO \cdot 6.6Al_2O_3)$, $\beta_{II} = BaAl_{9.2}O_{14.8}$, $(BaO \cdot 4.6Al_2O_3)$, tr = traces, (i) only most intense peaks visible, nd = not determined.

sample, the phase initially present was also microcrystalline boehmite (or pseudoboehmite) which became amorphous at about 400 °C. The transition aluminas that formed were γ-Al_2O_3 and θ-Al_2O_3 instead of just γ-Al_2O_3 as in the pure alumina sample. The transformation from θ-Al_2O_3 to α-Al_2O_3 began at about 1050–1100 °C. After calcination at 1000 °C for 1 hour traces of the $BaAl_{9.2}O_{14.8}$ (β_{II}) phase were present. After calcination for 1 hour at 1200 °C or 1400 °C, $BaAl_{13.2}O_{20.8}$ (β_I) was present instead of β_{II}. Calcination in argon or argon + air for 1 h at 1400 °C gave the same result.

In the autoclave treated alumina and alumina-baria precursor gels, XRD showed that the samples initially consisted of well-crystallised boehmite which decomposed at 450–500 °C to an amorphous phase. Two rather weak peaks corresponding to the main peaks in the spectrum for γ-barium carbonate were also detected. *In-situ* XRD showed that the two $BaCO_3$ peaks persisted to 700 °C at which temperature a peak corresponding to the main BaO peak appeared and transition alumina formed. After 1 h at 1000 °C, γ-Al_2O_3, δ-Al_2O_3 and BaO were the phases present. After 1 h at 1200 °C both γ-Al_2O_3 δ-Al_2O_3 and $BaAl_2O_4$ were present. After 1 h at 1400 °C, θ-Al_2O_3 and δ-Al_2O_3 were present with $BaAl_2O_4$ and $BaAl_{9.2}O_{14.8}$ (β_{II}). A trace amount of α-Al_2O_3 was found in this sample calcined in air for 1 h and after 10 h at 1400 °C θ-Al_2O_3 was still the predominant phase. However in samples calcined in argon for 1 h at 1400 °C the principle phase was α-Al_2O_3.

4.3. DTA/TG analysis

The DTA/TG curves in Fig. 2 for the hydrothermally treated baria-doped samples show well-defined exothermic peaks corresponding to the decomposition of boehmite by dehydroxylation. A displacement of the dehydroxylation peaks to higher temperatures with increased heating rate indicates the slow kinetics of dehydroxylation. The theoretical weight loss for the dehydroxylation of boehmite is 15%. In Ba doped boehmite a weight loss of less than 15% was expected whatever barium compound was present, e.g. carbonate or

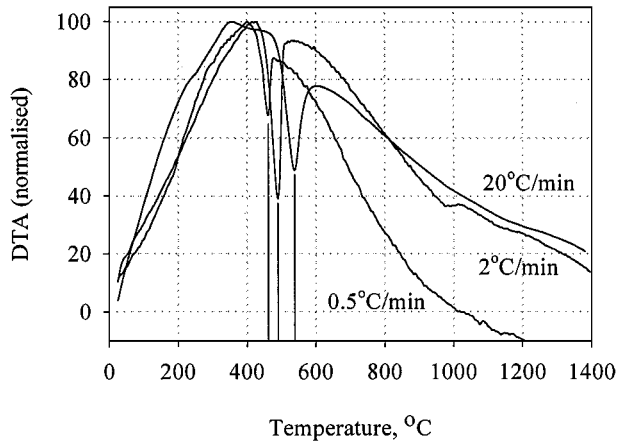

Figure 2 DTA analysis of autoclave treated alumina-baria precursor gel for various heating rates.

hydroxide, due to the high atomic weight of barium compared with aluminium. There was no indication of Ba phases such as $BaCO_3$ or $Ba(OH)_2 \cdot xH_2O$ which have a number of well-defined peaks by which they could easily be identified if present.

4.4. Surface area measurement

BET surface area measurements were made on samples calcined for 1 h at either 1200 °C or 1400 °C. For calcination at 1200 °C a value of 45.2 m^2/g was measured for specimens autoclaved for 4 h. For calcination at 1400 °C values of 5.9 m^2/g and 31.2 m^2/g were obtained for specimens autoclaved for 4 h and 22 h respectively. The longer autoclave treatment resulted in larger boehmite crystal size in the sample before calcination. After calcination at 1400 °C the phase composition of the specimens was also different. From XRD analysis, the phases present in order of abundance in the specimen autoclaved for 4 h were: θ-Al_2O_3, δ-Al_2O_3, $BaAl_2O_4$, and β_{II}. The specimen autoclaved for 22 h differed in that δ-Al_2O_3 was absent.

4.5. TEM/HRTEM examination

TEM examination showed that considerable morphological differences existed between ovendried,

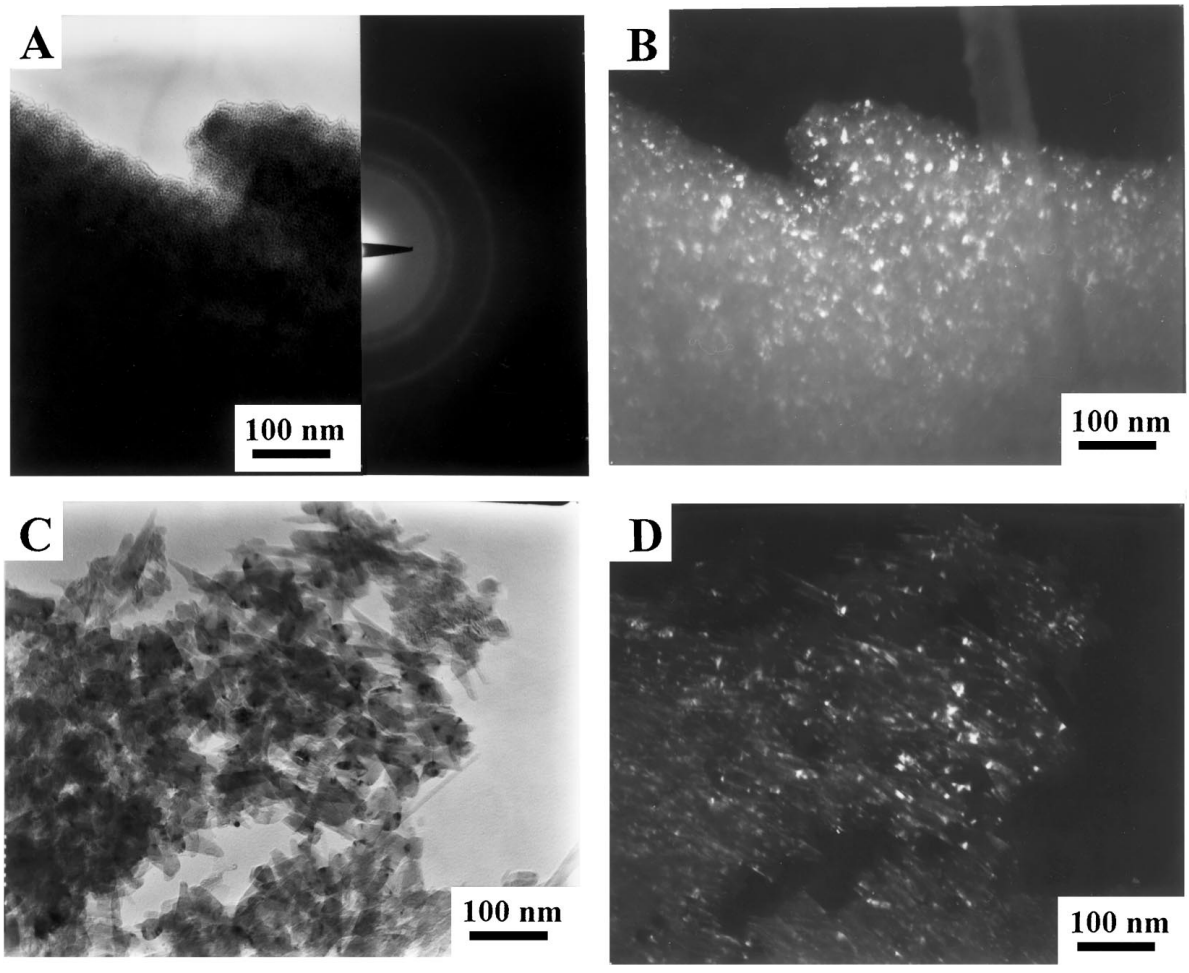

Figure 3 TEM micrographs of oven-dried alumina-baria precursor gel: (A) and (B) microcrystalline bayerite before calcination, bright and dark field respectively; (C) and (D) γ-Al_2O_3 with crystals of β_{II} after 1 h at 1000 °C, bright and dark field respectively.

microwave-dried and hydrothermally treated samples, both before and after calcination.

Before calcination, the oven-dried material consisted of densely agglomerated fine crystals, Fig. 3A and B, which were identified by electron diffraction as bayerite. The microwaved material was much less tightly agglomerated as shown in Fig. 4A and consisted of boehmite crystallites of about 5 nm as seen by HRTEM (not shown here) which approximately corresponded to the size of the colloidal particles in the gel. The hydrothermally treated sample consisted of plate-like boehmite crystals about $250 \times 100 \times 10$ nm as shown in Fig. 5A. There was no evidence of a separate Ba containing phase in any of the uncalcined samples.

TEM micrographs of oven-dried material calcined for 1 h at 1000 °C indicated the presence of a γ-Al_2O_3 matrix and finely distributed BaO (small dark particles)—see in Fig. 3C and D. The crystallite size of the γ-Al_2O_3 and barium containing phase was about the same after calcination as that of bayerite before calcination i.e. compare Fig. 3B and D. After calcination at 1000 °C the autoclaved material consisted of γ-Al_2O_3 which retained the shape of the boehmite crystals (pseudomorphs) as shown in Fig. 5B. The pseudomorphs were porous and the pore facets can be seen in Fig. 5C.

The TEM image of microwaved material calcined at for 1 h at 1200 °C, Fig. 4B, shows the start of the transition from θ-Al_2O_3 to α-Al_2O_3. After calcination at 1400 °C for 1 h in air or argon the microwaved material consisted $BaAl_{13.2}O_{20.8}$ (β_I) particles of 10–15 nm diameter and much larger α-Al_2O_3 crystals as shown in Fig. 4C–F. The β_I particles were predominantly within the α-Al_2O_3 crystals after calcination in air but were distributed both within and on the surface of the α-Al_2O_3 crystals after calcination in argon.

The autoclave treated material, calcination at 1400 °C in air, consisted mainly of finely twinned θ-Al_2O_3 with twin planes spaced about 5 nm apart as shown in Fig. 6. The boehmite pseudomorph crystal shape was still retained although the internal porosity was much less than at 1000 °C, and was more spherical in shape. The θ-Al_2O_3 twin planes were parallel to the long axis of the pseudomorphs, i.e. the boehmite ⟨001⟩ direction. There was no evidence of sintering between the crystals and their size was similar to that at 1200 °C. Small amounts α-Al_2O_3 were observed. Detailed HRTEM examination of transition alumina structures in the autoclave treated samples indicated that the fine twinning in θ-Al_2O_3 seen in the material calcined at 1400 °C probably resulted from the ordering of cation vacancies in δ-Al_2O_3 at lower temperatures [24]. In contrast, autoclave treated material, calcined at 1400 °C

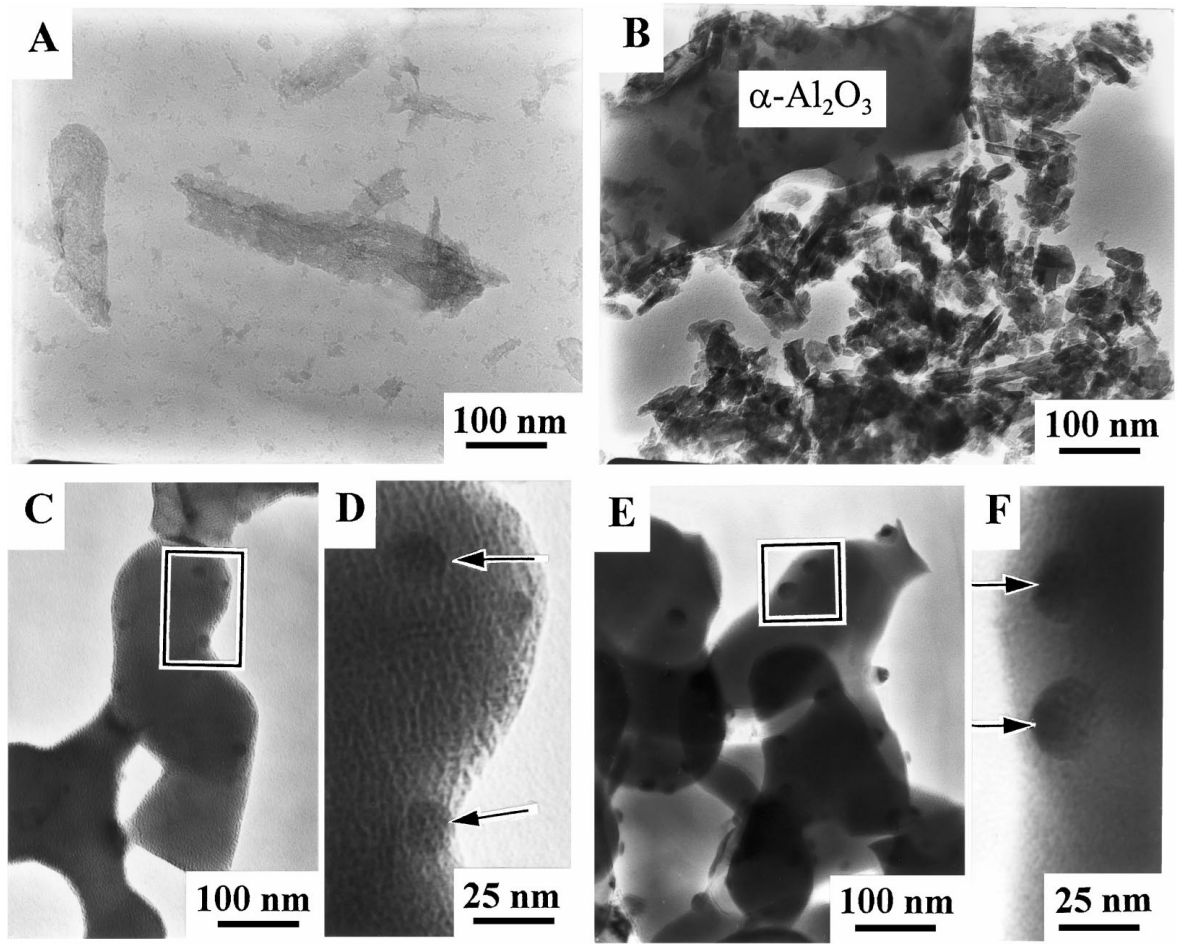

Figure 4 TEM micrographs of microwave treated alumina-baria precursor gel: (A) morphology after microwave drying, (B) large α-Al_2O_3 crystal growing in a matrix of θ-Al_2O_3 after 1 h at 1200 °C in air, (C) and (D) nano particles of β_I ($BaAl_{13.2}O_{20.8}$) phase inside α-Al_2O_3 crystals after 1 h at 1400 °C in air, (E) and (F) nano paticles of β_I inside and on the surface of α-Al_2O_3 crystals after 1 h at 1400 °C in argon.

in argon, consisted of large crystals of α-Al_2O_3 decorated on the surface with 10 nm particles of $BaAl_{12}O_{19}$ which has a magnetoplumbite structure rather than a β type structure—see Fig. 7.

5. Discussion

The most interesting findings in this work were the increased thermal stability of transition alumina in autoclave treated material, and the low temperature formation of β-aluminates in microwave treated samples. We interpret these phenomena in terms of the influence of the differences in the distribution of the barium dopant prior to calcination produced by different processing conditions. The processing conditions either tended to favour a uniform mixture of Ba and Al, i.e. in the case of microwave drying or oven drying, or they produced a distinct phase separation, i.e. in the case of autoclave treatment. The most effective technique for maintaining a uniform mixture of Ba and Al cations was microwave heating and this resulted in the early formation of aluminates. In contrast, autoclave treatment resulted in a phase separation which retarded the formation of β-aluminates and also retarded the transformation to α-Al_2O_3.

The barium doped gels were physically similar to those without barium. This was shown by SAXS measurements of particle size and fractal dimension. Barium appeared not to change either the size of primary particles or their state of aggregation. No barium containing phases could be detected by XRD, TEM or thermal analysis in the precipitated gels. Barium carbonate was detected by XRD in autoclave treated samples—although the peaks were rather weak—but these specimens consisted of boehmite rather than gel. In contrast, precipitation experiments in which barium was the only cation present yielded large agglomerates of well crystallised γ-barium carbonate (witherite). Pure barium carbonate and barium hydroxide—which is another possible reaction product—are easily identifiable by XRD, TEM and thermal analysis. These results suggest that most of the barium dopant was incorporated with the aluminium at a molecular level as an integral part of the amorphous gel structure, and that very little barium precipitated as a separate phase alongside the gel.

In the dried gels produced by oven-drying and microwave treatment we assume that the barium dopant was retained by the gel structure during drying. These dried gels were predominantly amorphous and contained only small amounts of bayerite and boehmite respectively. The concentration of barium in these gels would increase only slightly if small amounts of aluminium was lost from the gel due to the crystallisation

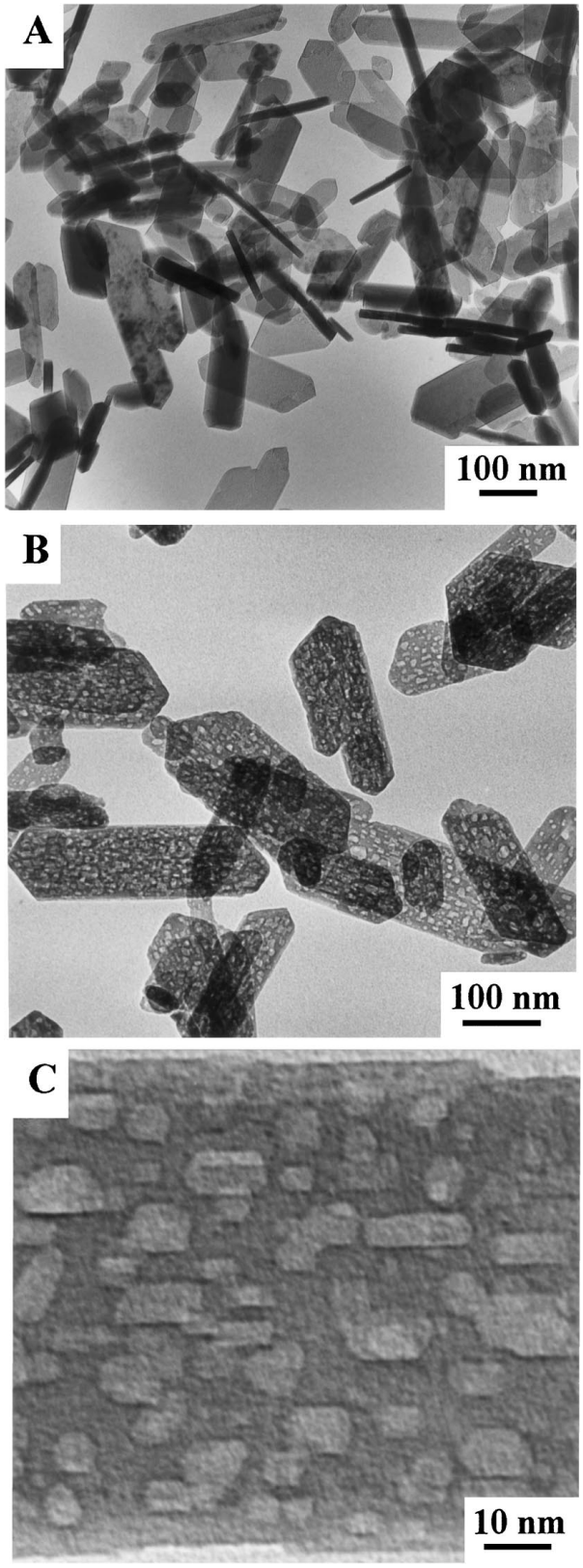

Figure 5 TEM micrographs of autoclave treated alumina-baria precursor gel: (A) well-developed boehmite crystals after hydrothermal treatment of 4 h at 210 °C, (B) porous boehmite pseudomorphs after 1 h at 1000 °C, (C) detail showing size, shape and orientation of pores.

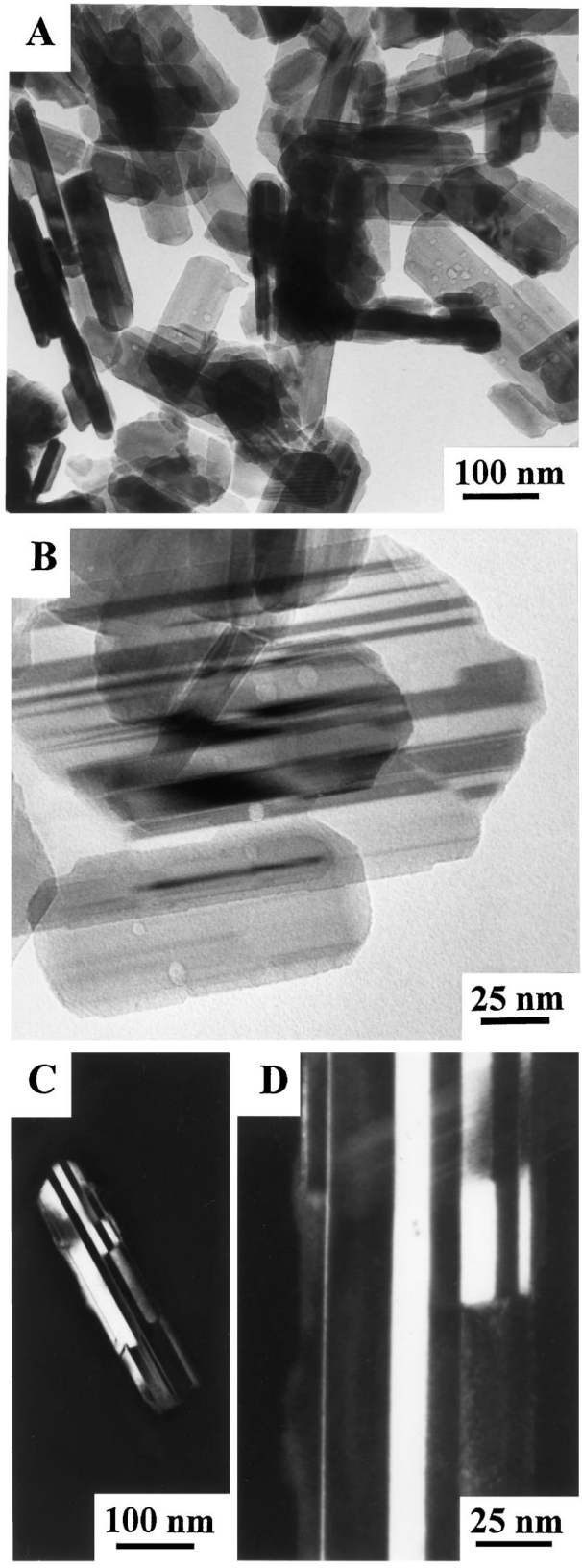

Figure 6 TEM micrographs of autoclave treated alumina-baria precursor gel after calcination for 1 h at 1400 °C in air: (A) boehmite pseudomorphs consisting of θ-Al_2O_3, (B) finely twinned θ-Al_2O_3 with equiaxed pores, (C) and (D) details of twinned θ-Al_2O_3 structure showing twin lamella as narrow as 5 nm.

of bayerite or boehmite. There was therefore only a small amount of phase separation in these materials.

Autoclave treated gels, however, appeared to consist entirely of well-formed crystals of boehmite according to our TEM images and the barium carbonate detected by XRD was not visible. There was no indication of any amorphous material remaining. However, calculation indicates that if all the barium existed as a uniform layer of barium carbonate on the surface of the 10 nm thick boehmite crystals, that layer would only be about

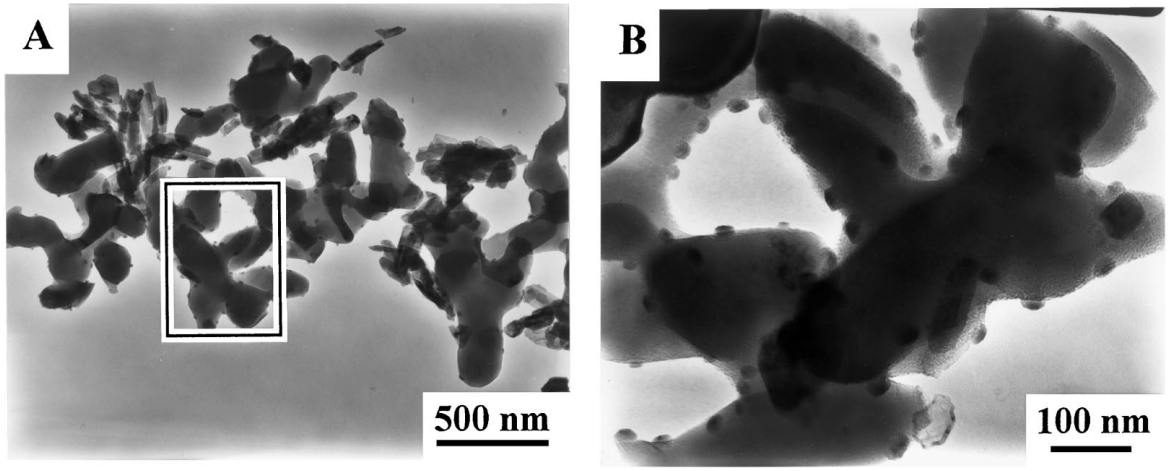

Figure 7 TEM micrographs of autoclave treated alumina-baria precursor gel after calcination for 1 h at 1400 °C in argon: (A) nano particles of $BaAl_{12}O_{19}$ in a matrix of θ-Al_2O_3 transformed extensively to α-Al_2O_3, (B) detail showing $BaAl_{12}O_{19}$ particles predominantly on the surface of α-Al_2O_3.

0.5 nm thick, which would be too thin to be seen by TEM. The only TEM images which showed separate Ba containing phases showed particles rather than layers, and these concerned specimens calcined at 1400 °C in which the alumina was present as α-Al_2O_3 e.g. Fig. 7B. In these cases, the Ba containing particles were easily visible and their concentration was so high that if such particles had been present in the same samples calcined at lower temperatures, or on boehmite before calcination, they would certainly be visible in TEM images. Crystalline boehmite and transition alumina were therefore shown to be associated with barium, but not in a form visible by TEM, perhaps as a thin surface layer. However, because we have no experimental evidence for such a layer, we must also consider the possibility that the barium dopant was incorporated into the boehmite structure.

It seems unlikely that barium was incorporated directly into the boehmite lattice by substitution because the ionic radius of barium ($Ba^{2+} = 0.134$ nm) is large compared with that of aluminium ($Al^{3+} = 0.051$ nm). Moreover, substitution of Al^{3+} by Ba^{2+} should produce changes in the XRD spectrum, but no such changes were observed; there was no peak broadening, no change in relative peak intensity, nor any shift in peak positions.

Intercalation layers might, however, provide suitable sites for the large Ba ions. Several intercalated forms of boehmite exist e.g. water intercalated (pseudoboehmite), ethylene glycol intercalated [28], and Li intercalated [29]. In these materials direct evidence of intercalation was provided either by precise identification of the lattice sites of the intercalated species or by a very large increase in the 020 spacing between boehmite layers. Pseudoboehmite was obtained from amorphous alumina gel, which is essentially $Al(OH)_3$, and the Li and ethylene glycol intercalated forms of boehmite were obtained by reaction with gibbsite, $Al(OH)_3$. We know of only one report of an intercalated boehmite derived from boehmite rather than from gibbsite [30] and this report concerned a copper acetate infiltrated boehmite for which no measurable increase in the boehmite layer spacing was found and for which no experimental evidence for intercalation was presented. Our amorphous gels were therefore plausible precursors for intercalated boehmite, but the XRD spectra for the autoclave treated barium doped material showed no change in 020 peak intensity nor any displacement of the peak to lower angles. No additional peaks were found at lower diffraction angles in the range measured i.e. down to $2\theta = 5°$, a value that corresponds to lattice spacing of 17.7 nm, which is almost 3 times that for non-intercalated boehmite. We therefore cannot provide evidence for intercalation in our materials and, by elimination, we favour the surface layer hypothesis for the location of the barium dopant. This type of layer could have formed by precipitation on cooling the autoclave. We conclude that autoclave treatment resulted in a complete phase separation between Al and Ba species.

An observation consistent with the hypothesis of a thin surface layer of the barium phase, as given above, is that after calcination at 1400 °C the autoclaved samples consisted of barium aluminate particles on the surface of the alumina crystals. In contrast, in the microwave treated samples the barium aluminate particles were uniformly distributed throughout the alumina matrix, which is consistent with the idea of atomic scale mixing of Ba^{2+} and Al^{3+} ions in the microwave treated specimens. In the autoclaved sample, BaO reacted at temperatures above 1000 °C to form barium aluminates on the surface of the alumina, whereas barium aluminates appeared to form directly at low temperatures in the microwave-dried specimen. The oven-dried specimens appeared to represent a case intermediate between microwave-dried and autoclaved specimens. The oven drying process seemed to result in a separation of the barium species, as shown by the appearance of BaO on calcination at 1000 °C. The BaO apparently did not form a surface layer as in the autoclaved specimens, however, but the barium phase was distributed uniformly throughout the alumina as seen from TEM images of the β_I particles inside α-Al_2O_3 crystals after calcination at 1400 °C. The importance of the distribution of the barium dopant can therefore be seen, firstly from the apparent correlation of a surface layer

of $BaAl_2O_4$ with a higher thermal stability of transition alumina in the autoclaved specimens compared with oven-dried samples, and secondly from the absence of $BaAl_2O_4$ in microwave treated samples in which β-aluminates formed directly at low temperature. These results show that the phase composition of the calcined alumina was determined by the initial distribution of the barium dopant, which in turn depended on how the gel was processed. Mechanisms by which the distribution of barium could results in the observed phase compositions are described below.

A surface layer of aluminate would be expected to influence the nucleation of α-Al_2O_3 from transition alumina. For example, in lanthanum doped alumina, a surface layer of $AlLaO_3$ was reported to form with an oxygen sublattice coherent with that of the underlying transition alumina, and which thereby eliminated anionic vacancy sites at the surface of the transition alumina [25, 27]. The effect of lanthanum doping was to increase the thermal stability of transition alumina because surface vacancy sites on transition alumina acted as nucleation sites for the transformation to α-Al_2O_3. However, Ba is not completely analogous with La as a dopant for two reasons. First, La can also stabilise transition alumina by forming a solid solution [31], but this seems excluded in the case of Ba due the large ionic size of Ba^{2+}, as mentioned above. Secondly, barium aluminate surface layers are more complex than lanthanum aluminate layers because several barium aluminates can form sequentially at intervals determined by the kinetics of diffusion [32].

The barium phase in the autoclaved treated samples transformed according to the sequence $BaO \rightarrow BaAl_2O_4 \rightarrow BaAl_{9.2}O_{14.8}$. Whereas the $BaO \rightarrow BaAl_2O_4$ transformation occurred at a temperature too low to be of significance for the stability of transition alumina, the $BaAl_2O_4 \rightarrow BaAl_{9.2}O_{14.8}$ transformation occurred at a temperature higher than is normal for the nucleation of α-Al_2O_3. The phase transformation in the barium aluminate system require a change in composition which occurs by diffusion. However because Ba^{2+} is a large ion, it is relatively immobile compared to the Al^{3+} and O^{2-} ions. The transformation $BaAl_2O_4 \rightarrow BaAl_{9.2}O_{14.8}$ therefore occurs by the capture of Al^{3+} and O^{2-} ions by $BaAl_2O_4$ from Al_2O_3. This process can be expected to create vacancies at the interface between the two phases, and thereby to create sites for the nucleation of α-Al_2O_3. The simultaneous transformation of transition alumina to α-Al_2O_3 and of $BaAl_2O_4$ to hexaluminate has been noted previously in the literature [3]. The thermal stability of transition alumina in autoclaved samples therefore seemed to depend on the resistance of the $BaAl_2O_4$ surface layer to transformation to higher aluminates. Although transition alumina derived from boehmite has a greater thermal stability than that from amorphous precursors [20, 26], the contribution of the surface layer of $BaAl_2O_4$ to thermal stability in our samples is demonstrated by comparing the results of calcining the autoclaved material in air and in argon. The argon atmosphere initiated an earlier transformation to α-Al_2O_3, presumably by accelerating the kinetics of diffusion in the $BaAl_2O_4 \rightarrow BaAl_{9.2}O_{14.8}$ transformation by the creation of additional oxygen vacancies at low oxygen partial pressure. It therefore appears that the surface layer of $BaAl_2O_4$ did increase the thermal stability of transition alumina against transformation to α-Al_2O_3 and that although the protection was limited by the tendency to transform to $BaAl_{9.2}O_{14.8}$, the $BaAl_2O_4$ was nevertheless more stable as a surface layer on the autoclave treated sample than as a nanoscale distribution of particles in the oven-dried sample.

6. Conclusions

Barium doped alumina gels were produced from inorganic salts by homogenous precipitation. Hydrothermal treatment of the gel before calcination resulted in transition alumina with improved thermal stability, capable of withstanding 1 h at 1400 °C in air without transformation to α-Al_2O_3. The increased thermal stability is attributed to a surface layer of $BaAl_2O_4$ on the alumina crystals. Microwave treatment of the gel before calcination resulted in formation of β-aluminates at relatively low temperatures and no increase in thermal stability of the transition alumina. The low temperature formation of aluminates in microwave treated gels is attributed to retention of molecular scale mixing of cations with this form of drying in contrast to conventional oven drying which resulted in phase separation and retarded the formation of barium aluminates.

Acknowledgements

We thank Mr. P. Thomas of University of Limoges, France for making the in-situ XRD measurements, and also Mr. P. Tambuyser and Mr P. Glaude of IAM, Petten, Netherlands for making the TEM and XRD analyses respectively.

References

1. D. L. TRIMM, *Appl. Catal.* **7** (1983) 249.
2. R. PRASAD, L. A. KENNEDY and E. RUCKENSTEIN, *Catal. Rev.-Sci. Eng.* **26** (1984) 1.c.
3. M. MACHIDA, K. EGUCHI and H. ARAI, *J. Catal.* **103** (1987) 385.
4. G. GROPPI, C. CRISTIANI, P. FORZATTI and M. BELOTTO, *J. Mater. Sci.* **29** (1994) 3441.
5. M. MACHIDA, K. EGUCHI and H. ARAI, *Bull. Chem. Soc. Jpn.* **61** (1988) 3659.
6. *Idem., Chem. Lett.* (1986) 151.
7. *Idem., ibid.* (1987) 767.
8. *Idem., J. Catal.* **120** (1989) 377.
9. S. KIMURA, E. BANNAI and I. SHINDO, *Mater. Res. Bull.* **17** (1982) 209.
10. N. IYI, S. TAKEKAWA, Y. BANDO and S. KIMURA, *J. Solid State Chem.* **47** (1983) 34.
11. N. IYI, S. TAKEKAWA and S. KIMURA, *ibid.* **83** (1989) 8.
12. N. IYI, Z. INOUE, S. TAKEKAWA and S. KIMURA, *ibid.* **52** (1984) 66.
13. *Idem., ibid.* **60** (1985) 41.
14. N. IYI, Y. BANDO, S. TAKEKAWA, Y. KITAMI and S. KIMURA, *ibid.* **64** (1986) 220.
15. A. R. WEST, *Mater. Res. Bull.* **14** (1979) 441.
16. A. L. N. STEVELS, J. Electrochem. Soc. **125** (1978) 588.
17. E. MATIJEVIĆ, Acc. Chem. Res. **14** (1981) 22.

18. *Idem.*, in "Ultrastructure Processing of Ceramics Glasses and Composites," edited by Mackenzie (Ulrich, Wiley, 1987) p. 429.
19. B. DJURIČIĆ, S. PICKERING, D. MCGARRY, P. GLAUDE, P. TAMBUYSER and K. SCHUSTER, *Ceram. International* **21** (1995) 195.
20. B. DJURIČIĆ, S. PICKERING, P. GLAUDE, D. MCGARRY and P. TAMBUYSER, *J. Mater. Sci.* **32** (1997) 589.
21. B. DJURIČIĆ, I. J. DAVIES, S. PICKERING, D. McGARRY, E. BULLOCK, M. VERWERFT, P. M. BRONSFELD and J. TH M. DE HOSSON, *Silicates Industriels* **60** (1995) 203.
22. B. DJURIČI,Ć S. PICKERING and D. McGARRY, *J. Mater. Sci. Lett.* **14** (1995) 1534.
23. J. TEIXEIRA, *J. Appl. Cryst.* **21** (1988) 781.
24. Y. G. WANG, P. M. BRONSFELD, J. TH. M. DE HOSSON, B. DJURIČIĆ, D. McGARRY and S. PICKERING.
25. S. KOMARNENI, V. C. MENON, Q. H. LI, R. ROY and F. AINGER, *J. Amer. Ceram. Soc.* **79** (1996) 1409.
26. F. OUDET, P. COURTINE and A. VEJUX, *J. Catal.* **114** (1988) 112.
27. R. K. ILER, *J. Amer. Ceram. Soc.* **47** (1964) 339.
28. M. INOUE, Y. KONDO and T. INUI, *Inorg. Chem.* **27** (1988) 215.
29. A. V. BESSERGUENEV, A. M. FOGG, R. J. FRANCIS, S. J. PRICE, D. OHARE, V. P. ISUPOV and B. P. TOLOCHKO, *Chem. Mater.* **9** (1997) 241.
30. V. PIERRE, D. PIERRE and C. A. PIERRE, *J. Mater. Res.* **10** (1995) 2271.
31. V. A. USHAKOV, R. A. SHKRABINA, N. A. KORYABKINA and Z. R. ISMAGILOV, *Kinetics and Catalysis* **38** (1997) 117.
32. L. PERIER-CAMBRY and G.THOMAS, *Solid State Ionics* **93** (1997) 315.

Received 28 July 1997
and accepted 13 November 1998